AIR MOVEMENT & VENTILATION CONTROL WITHIN BUILDINGS

12th AIVC Conference, Ottawa, Canada
24-27 September, 1991

PAPER 6

WIND INDUCED FLUCTUATING AIRFLOW IN BUILDINGS

JIWU RAO AND FARIBORZ HAGHIGHAT

CENTRE FOR BUILDING STUDIES
CONCORDIA UNIVERSITY
MONTREAL QUEBEC CANADA

ABSTRACT

Airflow through a building has both mean and fluctuating components due to spatial and temporal variations in wind-induced pressures. Most of the existing investigations consider the average values of wind pressures and predict steady-state solutions for airflow [1]. This paper presents some experimental results for the validation of a proposed fluctuating airflow model [2]. The new model employs spectral analysis and statistical linearization methods to model the pulsating airflow through buildings. Frequency information of wind pressures, spectral and co-spectra, in addition to mean values are used as inputs. The model calculates the frequency characteristics of resultant airflow and estimates the effects of fluctuations on total air exchanges. The fluctuating wind pressures and airflow are simulated in a laboratory experimental setup. The action of varying wind pressure is simulated by a controllable fan-damper unit. The experimentally estimated transfer functions and RMS values of airflow are compared with theoretical ones, good agreements are obtained.

LIST OF SYMBOLS

P^w, P^i, Q, ΔP: total wind-induced pressures, internal pressure, airflow through openings, and pressure differences across openings,

$\bar{P}^w$, $\bar{P}^i$, $\bar{Q}$, $\Delta\bar{P}$: steady-state components of above variables,

p^w, p^i, q, Δp: corresponding fluctuating components,

$P^w(\omega), P^i(\omega), Q(\omega), \Delta P(\omega)$: Fourier transforms,

$S_{p^w}(\omega), S_{p^i}(\omega), S_q(\omega), S^{(c)}_{p_1^w p_2^w}(\omega)$: spectra and co-spectrum,

K_1, K_2, n_1, n_2: flow coefficients and exponents,

A_1, A_2, L_1, L_2: opening cross areas and depths.

1. INTRODUCTION

Wind-induced pressures on building envelopes have both spatial and temporal variations due to the gustiness of the incoming wind and the interaction between wind and buildings. Existing research focuses on calculating the steady-state airflow due to average spatial variations of wind pressures, while increased interests have been drawn on the study of fluctuations in airflow through buildings due to temporal variations in wind pressures.

The fluctuating airflow through openings can be divided into two categories: eddy flow and pulsating flow. The eddy flow represents the

additional air exchange through an opening due to the penetration of eddies. The pulsating flow is the result of bulk flow caused by fluctuations in the pressure difference across the opening.

A method was proposed to use a spectral analysis method to calculate the pulsating airflow due to temporal and spatial variations of wind-induced pressures [2]. The fluctuating airflow is influenced both by the building characteristics, the resistance of the openings to flow, the inertia of the air mass in the openings and the compressibility of the room air, and by the frequency characteristics of wind pressures, their power spectra and the correlations among them. In this method, the mean and fluctuating airflows are calculated separately, and then are combined to predict the total airflow. This paper presents experimental validation results.

2. EXPERIMENTAL SETUP

The actions of varying wind pressures on a building and the resultant fluctuating airflow are simulated in an experimental setup. The setup includes the chamber, damper, tracer gas unit, sensors, and data acquisition system (Fig. 1).

The chamber has dimensions of 7.5'X15.5'X7.7' and a volume of 900 ft^3 (25 m^3). It is built of two 3/4" plywood boards and filled with vertical wood stud frames and fibre glass insulation. Two laminated doors and two small single-glazing peep-windows are located on the same facade of the chamber. The cracks are sealed with caulking compound from inside. A purpose-provided opening is placed through the chamber wall and is filled with straws. Parameters of flow equations for the opening and the chamber porosity are measured by fan pressurization tests. When the opening is sealed, the chamber has approximately 1/20 ach (air changes per hour) in 50 Pascal pressurization tests.

The fluctuating wind-induced pressure is simulated by the damper unit. It consists of a proportional controller, a servo motor and a rotary position sensor, a damper, a venturi tube and a flow meter, blower fans and some ϕ3" plastic tubes. This unit is connected to the opening on the outside end. The analog output signal of the data acquisition system to the controller turns the damper to a designated angle, so that only a certain amount of airflow is allowed to pass and a required pressure level is generated at the opening.

The tracer gas set consists of tracer gas cylinders, injection mass flow controller, sampling tubes and pumps, and a GC analyzer. SF_6 is used as the tracer gas. The gas chromatograph analyzer is programmed, with the assistance of a digital relay switch, to sample at 20 second intervals. Calibrations have

been carried out, and the relationship between GC reading and the SF_6 concentration derived. A 12 channel sampler, with auto switching capability, pumps sampling air to the GC analyzer.

Pressures are measured with digital micromanometers with build-in auto-zero facility. Pressure taps are placed near two ends of the opening and inside the chamber.

The data collection and damper control are performed by a data acquisition system. The system has a capability of measuring up to 96 thermalcouple input channels, 16 range-adjustable analog input channels with 12 bit accuracy, 16 digital 1-bit input channels, and providing four 0-10V analog output channels of 12 bit accuracy. The system has built-in programmable timers and software/hardware interrupts, and run BASIC-like programs.

3. THEORETICAL CALCULATIONS

The chamber is modelled as a single-zone building with two openings. Opening 1 is the purpose-provided opening, and opening 2 represents the total porosity of the chamber envelope. In the steady-state calculation, the mass balance for this building is governed by:

$$K_1\left(\bar{P}_1^w - \bar{P}^i\right)^{n_1} + K_2\left(\bar{P}_2^w - \bar{P}^i\right)^{n_2} = 0 \tag{1}$$

For the analysis of fluctuating components in the pressures and airflows, the pressure/force balances for both openings result in two nonlinear governing equations:

$$\frac{\rho L_i}{A_i}\frac{dq_i}{dt} + \left(\frac{1}{K_i}\right)^{\frac{1}{n_i}}\left[\left(\bar{Q}_i + q_i\right)^{\frac{1}{n_i}} - \left(\bar{Q}_i\right)^{\frac{1}{n_i}}\right] = p_i^w - \frac{\gamma P_a}{V}\int_0^t (q_1 + q_2)dt, \tag{2}$$

where i=1, 2, same for the following equations.

The nonlinear terms in the above equations are approximated to linear relations through a statistical linearization method [3] as:

$$f_i = \left(\frac{1}{K_i}\right)^{\frac{1}{n_i}}\left[\left(\bar{Q}_i + q_i\right)^{\frac{1}{n_i}} - \left(\bar{Q}_i\right)^{\frac{1}{n_i}}\right] \sim \lambda_i q_i \tag{3}$$

Therefore, a set of linear governing equations can be obtained:

$$M_i \frac{dq_i}{dt} + \lambda_i q_i - p_i^w - B \int_0^t (q_1 + q_2) dt \tag{4}$$

where $B = \gamma P_d / V$ and $M_i = \rho L_i / A_i$. The coefficients of λ_i have values such that the variances of f_i and $\lambda_i q_i$ in both sets of equations (2 & 4) are the same. Assuming normal distributions for airflow rates q_i, the λ_i values can be expressed as:

$$\lambda_i = \frac{1}{\sigma_{q_i}} \int_{-\infty}^{\infty} \left\{ \left(\frac{1}{K_i} \right)^{\frac{1}{n_i}} \left[\left(\bar{Q}_i + q_i \right)^{\frac{1}{n_i}} - \left(\bar{Q}_i \right)^{\frac{1}{n_i}} \right] \right\}^2 \frac{e^{-\frac{q_i^2}{2\sigma_{q_i}}}}{\sqrt{2\pi}\,\sigma_{q_i}} dq_i \tag{5}$$

The linear equations (4) are Fourier transformed into the frequency domain, and converted in matrix form as:

$$\begin{bmatrix} K_1\lambda_1 + j\omega M_1 + \dfrac{B}{j\omega} & \dfrac{B}{j\omega} \\ \dfrac{B}{j\omega} & K_2\lambda_2 + j\omega M_2 + \dfrac{B}{j\omega} \end{bmatrix} \begin{bmatrix} Q_1(\omega) \\ Q_2(\omega) \end{bmatrix} = \begin{bmatrix} P_1^w(\omega) \\ P_2^w(\omega) \end{bmatrix} \tag{6}$$

The transfer function matrix can be obtained as:

$$H(\omega) = \begin{bmatrix} H_{11}(\omega) & H_{12}(\omega) \\ H_{21}(\omega) & H_{22}(\omega) \end{bmatrix} = \begin{bmatrix} K_1\lambda_1 + j\omega M_1 + \dfrac{B}{j\omega} & \dfrac{B}{j\omega} \\ \dfrac{B}{j\omega} & K_2\lambda_2 + j\omega M_2 + \dfrac{B}{j\omega} \end{bmatrix}^{-1} \tag{7}$$

When the spectra of wind pressures and the co-spectrum between them are known, the spectra for the fluctuating airflows can be expressed as:

$$S_{q_i}(\omega) = |H_{i1}(\omega)|^2 S_{p_1^w}(\omega) + |H_{i2}(\omega)|^2 S_{p_2^w}(\omega) - 2|H_{i1}(\omega)||H_{i2}(\omega)| S^{(c)}_{p_1^w p_2^w} \tag{8}$$

The RMS values of the fluctuating airflow are obtained through integration of corresponding spectra over frequency, i.e.:

$$\sigma_{q_i}^2 = \int_0^{\infty} S_{q_i}(\omega)\, d\omega \tag{9}$$

Equations (5 & 9) show that λ_i and σ_{q_i} are functions of each other. Iterative procedures are employed to adjust λ_i and σ_{q_i} gradually, until both equations hold for one set of λ_i and σ_{q_i}.

The procedure for the theoretical calculation is as follows: first, the steady-state solution for the given building situation is obtained, and the initial set of σ_{q_i} is assumed; second, λ_i values are calculated for the current σ_{q_i} values; third, the transfer functions are calculated, spectra and RMS values are obtained; finally, the new σ_{q_i} are compared with the old values, and repeated from the second step if necessary.

4. EXPERIMENTAL PROCEDURE AND COMPARISON OF RESULTS

The experiment is conducted in the following manner: (1) A measured amount of tracer gas SF_6 is injected into the chamber and mixed for 10 minutes with a mixing fan. (2) During the mixing, a pressurization test is performed. The damper angle is increased or decreased step by step with a time lag between two steps to allow the flow to reach steady-state condition. The pressures and flow rate are monitored and data is used to calculate the flow relations of the opening and chamber porosity. This test is repeated several times during the experiment. (3) A program that generates a temporal fluctuating signal to the damper is executed, and data is collected at 5 Hz for about 45 minutes. (4) The damper is set at a constant angle to conduct a steady-flow decay test for around 30 minutes.

The fluctuating airflow data comes from step (3) of the test. The damper control signal is generated according to a certain spectrum. The collected data of external pressure, internal pressure, airflow rate and the control signal varys with time (Fig. 2). In the analysis, the data are examined in pairs of two such as external pressure ($p^w{}_1$) and airflow (q_1), external pressure and internal pressure (p^i), and, external pressure and pressure difference (Δp_1). The emphasis of validation is to compare the relationship within these pairs in the frequency domain.

For the external pressure ($p^w{}_1$) and airflow (q_1) pair, the spectra and transfer function are estimated using a smoothed Fourier transform spectral estimator with a sample length of 1024 data points and Hanning windows. The magnitude of the transfer function (Fig. 3c) shows a peak between 0.1 to 1 Hz, which is due to the inertia of air in the opening and the compressibility of room air. The fluctuating airflow model is implemented, on a case bases, in MATLAB [4] programs. In the theoretical calculation, the estimated external pressure spectrum, as well as the building characteristics and measured flow relations, are used as input. The calculation converges in four iterations to a precision of 10^{-7} when the experimental RMS values are used for initialization. The transfer function between $p^w{}_1$ and q_1 corresponds to $H_{11}(\omega)$ in the equation (7). If the calculated transfer function confirms with the measured one, the theoretical model will correctly predict the resultant airflow.

In Fig. 3c, the theoretical transfer function magnitude is plotted against the experimental results. It agrees well with the measured one for frequencies less than 0.3 Hz. At higher frequencies (>0.5 Hz), the measured curve shows very low values instead of reaching the peak as the theoretical results. This is probably due to the data quality. The coherence between p^w_1 and q_1 are low at higher frequencies (Fig. 4), thus, the estimated transfer function is inaccurate. A second possible explanation is that the assumption of inertia of air in the theoretical model is invalid for higher frequencies. Nevertheless, the power density of wind pressure is mainly concentrated at the low frequency range away from where the low coherence occurs. The resultant airflow at the high frequency range generally contributed very little to the total value. Therefore, the poor agreement between the experimental and theoretical transfer functions would not cause great inconsistency in the prediction.

The theoretical and experimental phase plots of the transfer function between p^w_1 and q_1 (Fig. 3d) are in good agreement. At low frequencies, the lag between q_1 and p^w_1 is negligible. The q_1 is ahead of p^w_1 in frequency 0.02 to 1.0 Hz due to the inertia of air in the opening. At high frequencies greater than 2 Hz, the inertia makes q_1 lag behind p^w_1.

Above calculations are also performed on the other pairs of data. In Fig. 5, the magnitude and phase plots of both estimated and calculated transfer functions for p^w_1 and p^i ,and, p^w_1 and Δp show very good agreements.

The theoretically calculated mean and RMS (root-mean-square) values of q_1, p_i, and Δp_1 are listed in Table 1. The calculated mean values match those of measured ones well as expected, since experimentally measured flow equations of the opening and porosity of the chamber are used as input. The calculated RMS values of fluctuating components also match within a 7% relative error range with the test results.

Figure 6 shows the results of the tracer gas decay conducted during the test step 3. The fitting result indicates an effective mean air infiltration of 6.5 l/s, or 85% of the mean airflow rate through the opening.

5. Discussions

Experiments are performed to validate a fluctuating airflow model which considers the pulsating airflow due to the temporal variations in wind pressures. The comparison of transfer functions and RMS values between experimental estimations and theoretical calculations show good agreement, especially in the low frequency range (<0.5 Hz). At the high frequency range, discrepancies exist between experimental and theoretical results, but the effect on predictions is minimized.

The theoretical model has not considered eddy flows whose effects on airflow are significant especially for large openings or single-sided ventilation. The argument for the omission is that the eddy flow is a more isolated phenomena, it depends mainly on the local flow field near the openings. A generalized analysis is more difficult than for the pulsating flow. In the experiment, the airflow is limited to pulsating by using straws in the opening.

ACKNOWLEDGEMENTS

Financial support through research grants from the Department of Energy, Mines and Resources of Canada and from the Natural Sciences and Engineering Research Council of Canada is acknowledged with thanks.

REFERENCES

1. F. Haghighat, "Air Infiltration and Indoor Air Quality Models - A Review", *The International J. of Ambient Energy*, Vol. 10, No. 3, pp 115-122.
2. F. Haghighat, J. Rao, and P. Fazio, "The Influence of Turbulent Wind on Air Change Rates - a Modelling Approach", *Building and Environment*, Vol. 26, No.3, pp 95-105, 1991.
3. V. V. Bolotin, *Random Vibration of Elastic Systems*, Translated by I. Shenkman, and H. Leipholz, Martinus Nijhoff Publishers, Boston, 1984.
4. C. Moler, J. Little and S. Bangert, *PRO-MATLAB for VAX/VMS Computers, Version 3.1-VMS*, The MathWorks, Inc., 1987.

Table 1. Experimental and Theoretical Results

	Experimental		Theoretical	
	Mean	RMS	Mean	RMS
Opening	$0.7467\ \Delta p^{0.80} \times 10^{-3}$ m^3/s		input	
Porosity	$0.3264\ \Delta p^{0.80} \times 10^{-3}$ m^3/s		input	
p^w_1 (Pascal)	64.6613	17.7177	input	
p^i (Pascal)	47.0775	12.6139	47.0716	12.3003
Δp_1 (Pascal)	17.5938	6.6735	17.5900	6.4239
q_1 ($\times 10^{-3}$ m^3/s)	7.6763	2.1314	7.6755	2.2732
q_2 ($\times 10^{-3}$ m^3/s)	7.6763	*	7.7655	1.6396
(q_1+q_2) ($\times 10^{-3}$ m^3/s)	*	*	0.0	2.2346
Decay Test	0.9235 ach 6.537×10^{-3} m^3/s		*	

* Not measured or calculated.

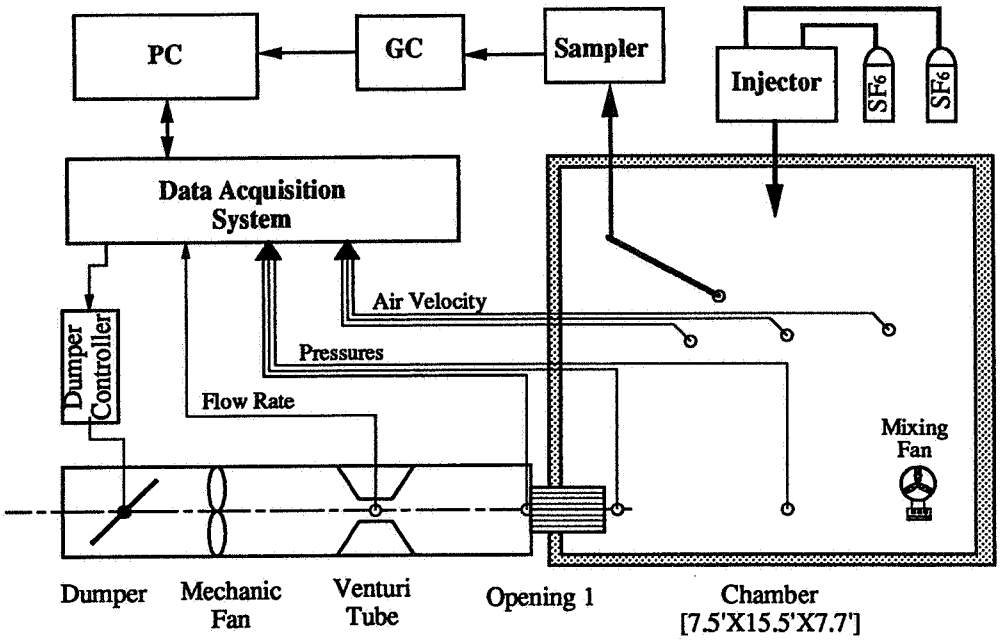

Figure 1. Experimental Setup

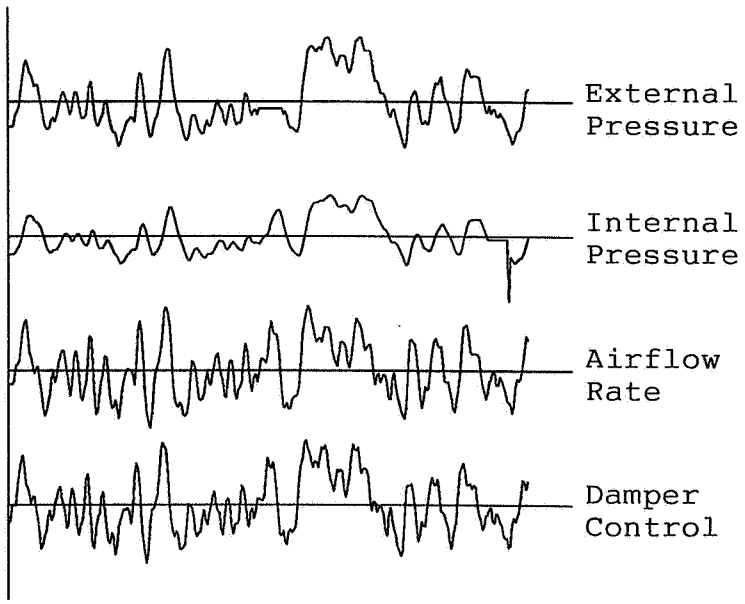

Figure 2. Experimental Data in the First Minute

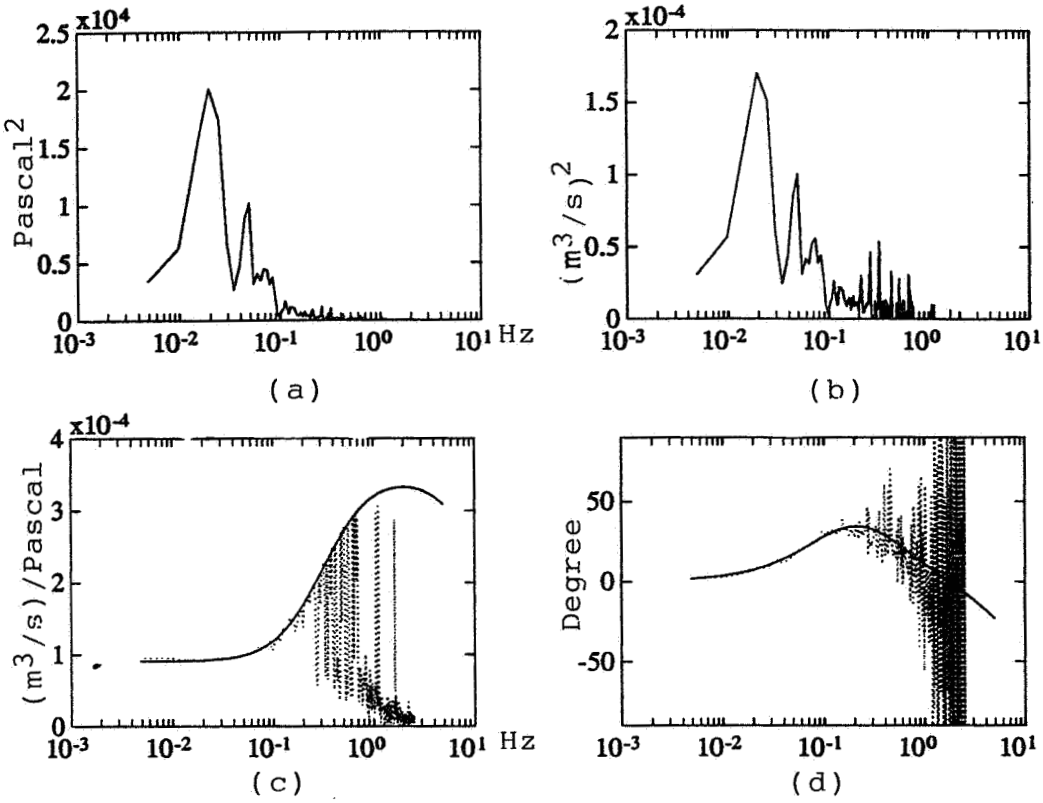

Figure 3. Frequency Results of External Pressure and Airflow: (a) External Pressure Spectrum, (b) Airflow Rate Spectrum, (c) & (d) Transfer Function

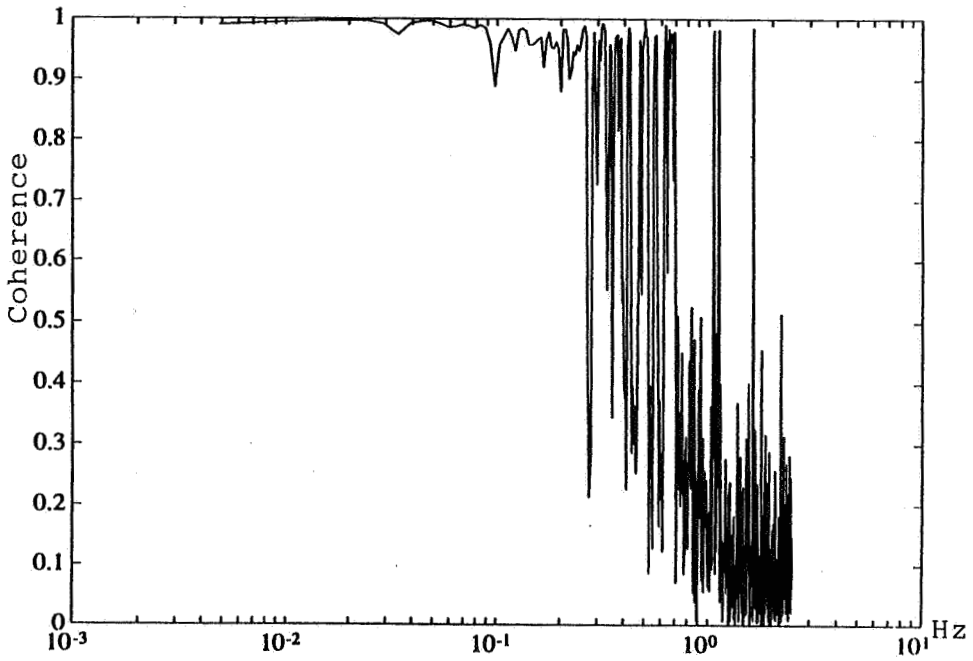

Figure 4. Coherence Between External Pressure and Airflow

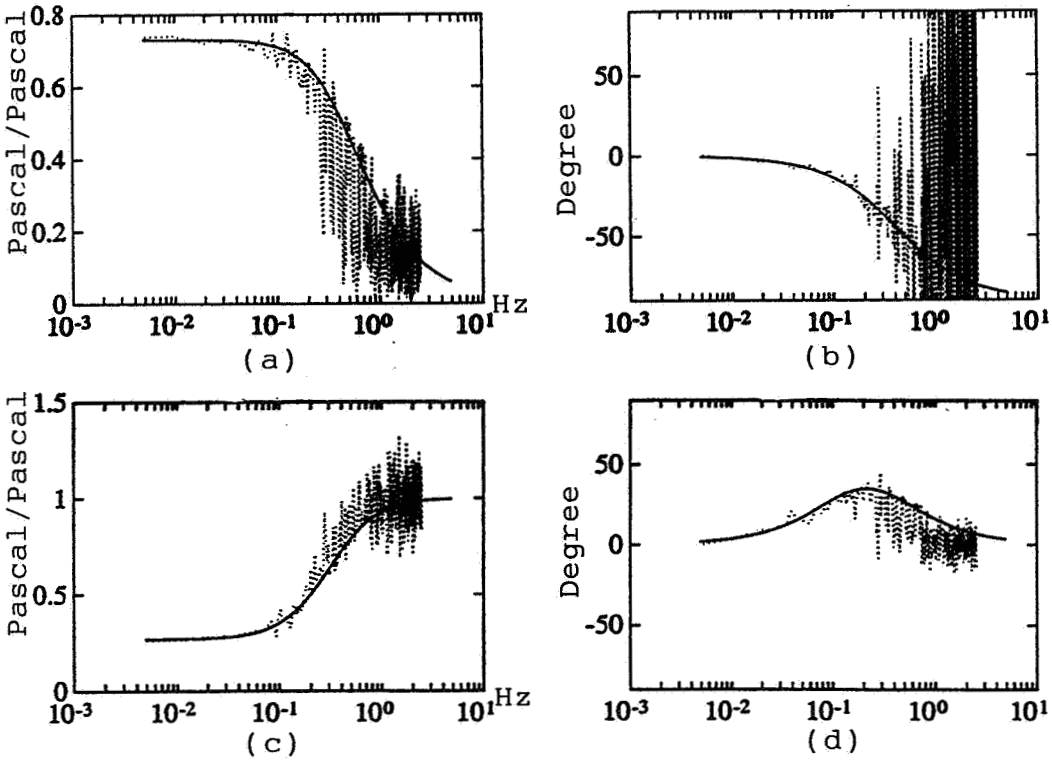

Figure 5. Magnitude and Phase Plots of Transfer Functions:
(a) & (b) External Pressure and Internal Pressure,
(c) & (d) External Pressure and Pressure Difference

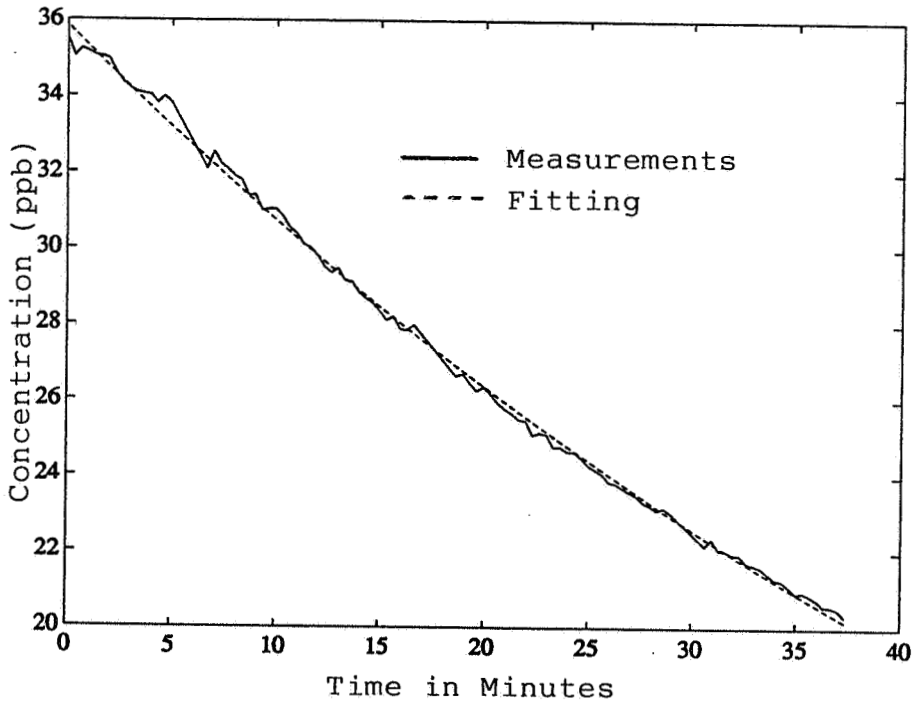

Figure 6. Tracer Gas Decay Test Results